Electronic Supporting Information for Extended conjugation in poly(triarylamine)s: Synthesis, structure and impact on field-effect mobility

By *Reiner Sebastian Sprick*, *Mario Hoyos*, *Marion Sofia Wrackmeyer, Adam Valentine Sheridan Parry, Iain Grace*, *Colin Lambert*, *Oscar Navarro** and *Michael Lewis Turner**

Prof. Michael L. Turner, R. Sebastian Sprick, Dr Marion Sofia Wrackmeyer, Adam Valentine Sheridan Parry
Organic Materials Innovation Centre, School of Chemistry, The University of Manchester, Oxford Road, Manchester, M13 9PL (United Kingdom).
E-mail: michael.turner@manchester.ac.uk; Fax: (+44) 0161 275 4273

Dr Mario Hoyos
Instituto de Ciencia y Tecnología de Polímeros, ICTP-CSIC, c/Juan de la Cierva, 3, Madrid, 28006 (Spain). E-mail: hoyos@ictp.csic.es; Fax: (+34) 91 564 48 53.

Dr Oscar Navarro
Department of Chemistry, University of Sussex, Brighton, BN1 9QJ, (United Kingdom).
E-mail: O.Navarro@sussex.ac.uk; Fax: (+44) 01273 678734.

Dr Iain Grace, Prof. Colin Lambert
Department of Physics, Lancaster University, Lancaster, LA1 4YB (United Kingdom).
E-mail: i.grace@lancaster.ac.uk; Fax: (+44) 0152 484 4037.

General remarks

All reagents were obtained from commercial sources and used as received. Solvents were dried according to standard procedures or using an Innovative Technology PureSolv MD 7 system using aluminium oxide columns. Reactions were carried out under an argon atmosphere using standard Schlenk techniques. Flash column chromatography was performed on Fluorochem silica gel 60 Å (40-63 μm). ^{1}H and $^{13}C\{H\}$ NMR spectra were recorded at 400 and 100 MHz, respectively, on a Bruker Avance AV 400 MHz Ultrashield spectrometer in the solvent stated at 25 ºC. All spectra are referenced to the residual solvent peak. Elemental analysis was performed using a Carlo Erba Instruments EA1108 elemental analyser. GC-MS was performed on a HP5890 series II GC connected to a HP 5971A EI mass spectrometer. MALDI-TOF mass spectrometry was carried out using a Shimadzu Biotech AXIMA Confidence MALDI mass spectrometer in linear (positive) mode, referencing against PPG or PEG standards (4K-12K Da). Static contact angle measurements with the sessile drop method were recorded and analysed at room temperature on a Krüss DSA100 instrument measured in at least three different locations with water and iodomethane. UV-Vis absorption spectra were recorded on a Varian Cary 5000 UV-Vis-NIR spectrophotometer in dichloromethane at room temperature. Fluorescence spectra were recorded on a Varian Cary Eclipse fluorimeter in dichloromethane solution at room temperature. Cyclic voltammetry was performed in dichloromethane solution scanning at 100 $m \cdot V \cdot s^{-1}$ on a BASI Epsilon electrochemical workstation with a three-electrode cell, $Ag/AgNO_3$ (in dichloromethane:acetonitrile 1:1) as reference electrode, platinum wire as counter electrode and working electrode, in nitrogen-purged, 0.1 M solution of tetrabutylammonium hexafluorophosphate $[(C_4H_9)_4N]PF_6$ as a supporting electrolyte at room temperature. Wafers with a 300 nm SiO_2 layer on n^{++} Si were obtained from Si-Mat GmbH (Germany). Differential scanning calorimetry measurements were recorded using a Perkin Elmer Jade DSC instrument under nitrogen atmosphere, 5–10 mg of the sample was sealed in an aluminium pan with a crimping tool. The sample was heated from 30 ˚C to 220 ˚C or 350 ˚C at a heating rate of 10 ˚C min^{-1}, held for 2 minutes at 220 ˚C or 350 ˚C and then cooled to 30 ˚C at a rate of 10 ˚C min^{-1}. This cycle was repeated once. WAXS spectra were recorded on a Bruker AXSAXS D8 Discover using the precipitated polymers or spin-coated on a WSi_2-C coated silicon wafer.

Materials

6,6',12,12'-Tetra-*n*-octyl-6,12-dihydroindeno[1,2*b*]fluorene,[1,2] 6,6,12,12,15,15-hexa-*n*-butyl-

12,15-dihydro-6*H*-cyclopenta[1,2-*b*:5,4-*b*']difluorene,[3] 2,7-dibromocarbazole,[4] 3,9-dibromo-5,11-di-*n*-octylindolo [3,2-*b*]carbazole[5] and (IPr)Pd(allyl)Cl[6] were synthesized using literature procedures.

Monomer synthesis

2,8-Dibromo-6,6',12,12'-tetra-n-octyl-6,12-dihydroindeno[1,2b]fluorene

Bromine (0.04 mL, 0.711 mmol) in dichloromethane (10 mL) was slowly added to a solution of 6,6',12,12'-tetra-*n*-octyl-6,12-dihydroindeno[1,2*b*]fluorene (0.200 g, 0.28 mmol) in dichloromethane (40 mL) and stirred overnight under protection from light. Sodium thiosulfate (2 M aqueous solution, 5 mL) was added, the aqueous and organic phases were separated and the organic layer dried over $MgSO_4$ and filtered. Solvents were removed *in vacuo* and the crude product was purified by column chromatography (*n*-hexane on SiO_2) followed by recrystallization from ethanol yielding a white solid (0.215 g, 88%). ^{1}H NMR (400 MHz, $CDCl_3$): δ (ppm) = 7.58 (dd, *J* = 7.5 Hz and 2.0 Hz, 2H), 7.55 (s, 2H), 7.48-7.44 (m, 4H), 1.98 (t, *J* = 8.5 Hz, 8H), 1.18-1.03 (m, 40H), 0.79 (t, *J* = 7.0 Hz, 12H), 0.66-0.55 (m, 8H). ^{13}C{H} NMR (100 MHz, $CDCl_3$): δ (ppm) = 153.34, 147.51, 140.30, 139.89, 129.84, 126.12, 120.88, 120.77, 113.97, 55.11, 40.49, 31.79, 29.91, 29.20, 22.59, 14.07. m.p.: 86-87 ˚C. Anal. Calcd for $C_{52}H_{76}Br_2$: C, 72.54; H, 8.90; Br, 18.56%. Found: C, 72.59; H, 8.79; Br, 18.57%. MALDI-TOF MS: m/z Calcd for $C_{52}H_{76}{}^{81}Br^{79}Br$: 861.0 ($M^+$); found: 861 (100%).

2,10-Dibromo-6,6,12,12,15,15-hexa-n-butyl-12,15-dihydro-6H-cyclopenta[1,2-b:5,4-b'b'] difluorene

6,6,12,12,15,15-Hexa-*n*-butyl-12,15-dihydro-6*H*-cyclopenta[1,2-*b*:5,4-*b*']difluorene (400 mg, 0.59 mmol) was dissolved in dichloromethane (20 mL) under protection from light. Bromine (235 mg, 1.47 mmol, in 3.75 mL dichloromethane) was added and stirred overnight. Sodium thiosulfate (2 M aqueous solution, 5 mL) was added, the aqueous and organic phases were separated and the organic layer was dried over $MgSO_4$ and filtered. The solvents were removed *in vacuo* and the product was purified by column chromatography (petroleum ether 40-60 °C on SiO_2) to give product as a white solid (433 mg, 85%). ^{1}H NMR (400 MHz, $CDCl_3$): δ (ppm) = 7.64 (s, 2H), 7.62 (d, *J* = 8.5 Hz, 2H), 7.59 (s, 2H), 7.50-7.46 (m, 4H), 2.07-2.00 (m, 12H), 1.17-1.05 (m, 12H), 0.72-0.63 (m, 30H). ^{13}C{H} NMR (100 MHz, $CDCl_3$): δ (ppm) = 153.34, 150.74, 149.84, 141.17, 140.52, 139.24, 129.82, 126.19, 120.80, 120.49, 114.07, 113.75, 55.01, 54.30, 40.71, 40.35, 26.08, 26.00, 23.10, 13.87. m.p.: 219-

222 ˚C. Anal. Calcd for $C_{51}H_{64}Br_2$: C, 73.20; H, 7.71%; Br, 19.10. Found: C, 72.90; H, 7.72%. MALDI-TOF MS: m/z Calcd for $C_{51}H_{64}{}^{81}Br^{79}Br$: 836.3 ($M^+$); found: 836 (100%).

2,7-Dibromo-N-(n-octyl)carbazole

2,7-Dibromocarbazole (1.62 g, 4.98 mmol) was dissolved in DMF (15 mL, anhydrous). NaH (0.168 g, 7.01 mmol, 60% in mineral oil) was added in small portions to the reaction mixture and the resulting suspension was stirred for 30 minutes at room temperature. 1-Bromooctane (1.2 mL, 6.5 mmol) was added and the reaction was stirred overnight at room temperature. The reaction was quenched with H_2O (10 mL) and extracted with dichloromethane. The combined organic fractions were dried over $MgSO_4$, filtered and the solvents were removed under reduced pressure. The crude product was purified by column chromatography (petroleum ether 40-60 °C: ethyl acetate 9:1 on SiO_2) to give product as a white solid (1.99 g, 91 %). ^{1}H NMR (400 MHz, $CDCl_3$): δ (ppm) = 7.89 (d, *J* = 8.0 Hz, 2H), 7.53 (d, *J* = 2.0 Hz, 2H), 7.34 (dd, *J* = 8.0, 2.0 Hz, 2H), 4.19 (t, *J* = 7.0 Hz, 2H), 1.88 – 1.79 (m, 2H), 1.41 – 1.20 (m, 10H), 0.88 (t, *J* = 7.0 Hz, 3H). ^{13}C{H} NMR (100 MHz, $CDCl_3$): δ (ppm) = 141.50, 122.65, 121.63, 121.41, 119.82, 112.15, 43.50, 31.92, 29.43, 29.30, 28.91, 27.32, 22.76, 14.23. m.p.: 66-70 ˚C (Lit. m.p.: 66-67 ˚C).[7] Anal.Calcd for $C_{20}H_{23}Br_2N$: C, 54.94; H, 5.30; N, 3.20; Br, 36.55%. Found: C, 55.21; H, 5.36, N, 3.18%. GC-MS (EI): m/z calcd for $C_{20}H_{23}{}^{79}Br^{81}BrN$: 437.0 ($M^+$); found: 437.2.

DFT calculations

Electronic structure calculations were performed to find the ground state geometries and electronic band gap of oligomers based on polymer **1**-**8**, with the aliphatic side chains were shorted to methyl groups, using the DFT code Siesta.[8] The code uses an atomic orbital basis set and norm-conserving pseudopotentials. Here we use the generalized gradient approximation (GGA) to describe the exchange correlation functional and a double-ζ basis set was used to span the valence orbitals, this is sufficient to achieve basis set convergence. An energy cut-off of 150 Rydbergs was used to define the real space grid and the unit cell of the polymers was taken to be a dimer of the units shown in **Fig. 2**. The ground state geometry was then calculated by relaxing the system until all the forces on the atoms were less than 0.01 V·Ang^{-1}. The length of the relaxed unit cell is shown in **Table 3**.

The theoretical characterizations of the charge transport properties of organic materials are well described by Brédas.[9] The reorganization energies can be estimated, with

an adiabatic process, in this procedure the total adiabatic reorganization energy ($\lambda_{total} = \lambda_N + \lambda_C$) is a sum of the relaxation or reorganization energies given in Eqs. (1) and (2)

$$\lambda_N = E_N\,(rel) - E_N \tag{1}$$

$$\lambda_C = E_C\,(rel) - E_C \tag{2}$$

where $E_N(rel)$ and $E_C(rel)$ are the energies of the neutral state in the optimized (relaxed) geometry of a charged (cationic or anionic) molecule and the energies of a charged state in the optimized geometry of a neutral molecule, respectively. E_N and E_C are the energies of the neutral state in the optimized geometry of a neutral molecule and the energies of the charged state in the optimized geometry of a charged molecule, respectively.

Fabrication of bottom-gate top-contact OFET devices on Si/SiO$_2$

Wafers of highly doped n^{++} silicon on which a 300 nm thick oxide layer had been thermally grown were cut into 1 × 1 cm pieces and cleaned by washing and ultrasonication for 5 minutes with deionized water, acetone, methanol and 2-propanol. These substrates were then exposed to UV/ozone for 20 minutes and 75 µL of *n*-octadecyltrichlorosilane in 1,1,2-trichloroethane (3 mM solution) was spin-coated at 3000 rpm for 10 seconds on the cleaned substrates. This was repeated twice before the substrates were heated for 20 minutes on a hotplate in ambient conditions. Substrates were further cleaned by wiping off any excess *n*-octadecyltrichlorosilane with a methanol soaked tissue and this cleaning was followed by rinsing and ultrasonication with 2-propanol and acetone. The contact angle was checked using a drop of deionized water before spin-coating 100 µL of the polymer solution (10 mg mL^{-1} in 1,1,2-trichloroethane, filtered using a 0.45 µm syringe filter) at 3000 rpm for 60 seconds under ambient conditions. Substrates were dried at 80 ˚C for 2 hours before gold source and drain electrodes (50 nm) were thermally evaporated under high vacuum conditions (<10^{-6} Torr) on the organic semiconductor layer through a shadow mask with multiple devices of channel width of 2000 µm and channel length of 60 µm.

Fabrication of top-gate bottom-contact OFET devices on glass

Glass pieces (2 × 2 cm) were washed and ultrasonicated with 2-propanol, methanol and acetone. After drying the substrates were treated with UV/ozone for 20 minutes before

thermally evaporating chromium (3 nm) and gold source and drain electrodes (20 nm) under high vacuum conditions (<10^{-6} Torr) through a shadow mask with a channel width (W) of 1000 μm and a channel length (L) of 60 μm. The substrates were rinsed with methanol and treated with UV/ozone for 20 minutes before immersing them in a solution of 2,3,4,5,6-pentafluorothiophenol in ethanol (1 mM) for 24 hours. The substrates were rinsed with ethanol and dried on a hot-plate in air for 20 minutes. The polymer solution (200 μL, 10 mg·mL^{-1} solution in 1,1,2-trichloroethane, filtered using a 0.45 μm syringe filter) was spin-coated at 3000 rpm for 60 seconds under ambient conditions. Substrates were heated to 80 ˚C for 2 hours before spin-coating CYTOP (200 μL, 9 wt.% solution in perfluorotributylamine) at 3000 rpm for 60 seconds under ambient conditions. Substrates were dried for 40 minutes at 100 ˚C and an aluminium top-gate (60 nm) was thermally evaporated under high vacuum conditions (<10^{-6} Torr) on the substrate through a shadow mask. The source and drain contacts were isolated by isotropic argon plasma etching.

OFET Characterization

FET properties were measured using an Agilent E5270B precision measurement mainframe coupled to an Agilent E5287A atto level High Resolution Module. Contacts were made using Karl Süss PH100 manual microprobes. Output characteristics were obtained at a constant gate voltage V_G = -60, -40, -20, and 0 V and transfer characteristics at a constant drain voltage V_{SD} = -60 V, varying the gate voltage from +20 V to -60 V. The saturated hole mobility and the threshold voltage were calculated from a plot of the square root of the drain current versus gate voltage according to the following equation:

$$I_D = \frac{\mu_{FET} W C_i}{2L} (V_G - V_{Th})^2 \quad (1)$$

Where W is the width of the channel, L the length of the channel, C_i the equivalent capacitance of the dielectric (Si/SiO_2/OTS: 10 nF cm^{-2}, CYTOP: 2.1 nF cm^{-2})[10] and V_{Th} the threshold voltage. Measurements were performed at room temperature in air in the dark. The capacitance for Si/SiO_2/OTS substrates was determined by measuring representative MIM (metal-insulator-metal) capacitors on an Agilent E4981A capacitance analyser.

References

(1) Setayesh, S.; Marsitzky, D.; Müllen, K. *Macromolecules* **2000**, *33*, 2016–2020.

(2) Poriel, C.; Liang, J.-J.; Rault-Berthelot, J.; Barrière, F.; Cocherel, N.; Slawin, A. M. Z.; Horhant, D.; Virboul, M.; Alcaraz, G.; Audebrand, N.; Vignau, L.; Huby, N.; Wantz, G.; Hirsch, L. *Chem. A Eur. J.* **2007**, *13*, 10055–10069.

(3) Zheng, Q.; Gupta, S. K.; He, G. S.; Tan, L.-S.; Prasad, P. N. *Adv. Funct. Mater.* **2008**, *18*, 2770–2779.

(4) Dierschke, F.; Grimsdale, A. C.; Müllen, K. *Synthesis* **2003**, 2470–2472.

(5) Boudreault, P.-L. T.; Wakim, S.; Blouin, N.; Simard, M.; Tessier, C.; Tao, Y.; Leclerc, M. *J. Am. Chem. Soc.* **2007**, *129*, 9125–9136.

(6) Navarro, O.; Nolan, S. P. *Synthesis* **2006**, 366–367.

(7) Bouchard, J.; Wakim, S.; Leclerc, M. *J. Org. Chem.* **2004**, *69*, 5705–5711.

(8) Soler, J. M.; Artacho, E.; Gale, J. D.; García, A.; Junquera, J.; Ordejón, P.; Sánchez-Portal, D. *J. Phys. Condens. Matter* **2002**, *14*, 2745–2779.

(9) Brédas, J.-L.; Beljonne, D.; Coropceanu, V.; Cornil, J. *Chem. Rev.* **2004**, *104*, 4971–5004.

(10) Smith, J.; Hamilton, R.; McCulloch, I.; Heeney, M.; Anthony, J. E.; Bradley, D. D. C.; Anthopoulos, T. D. *Synth. Met.* **2009**, *159*, 2365–2367.

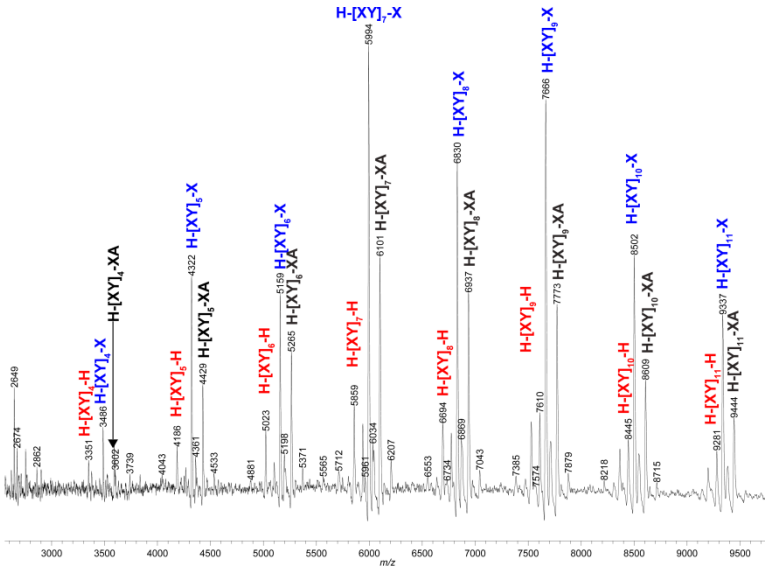

Figure-S 1 MALDI-TOF MS of **2**. X = 2-methyl-4-methoxy aniline, Y = indenofluorene and A = anisole.

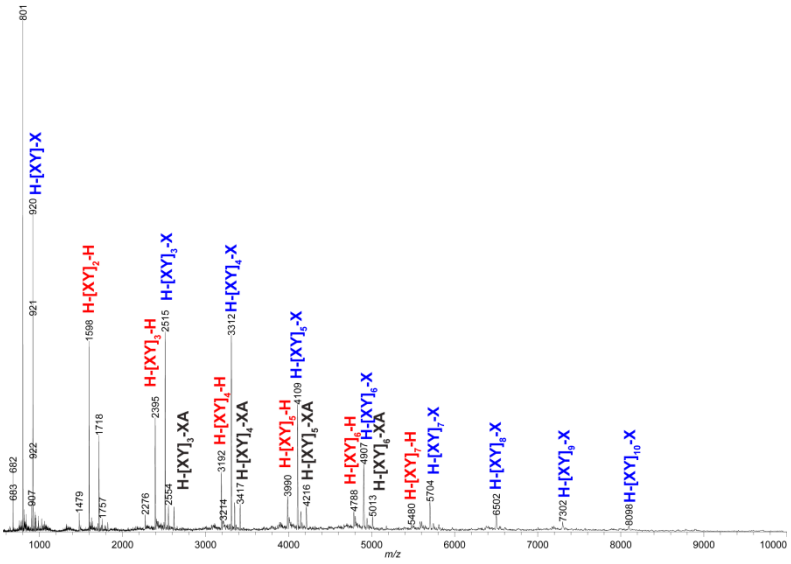

Figure-S 2 MALDI-TOF MS of **3**. X = 2-methyl-4-methoxy aniline, Y = diindenofluorene and A = anisole.

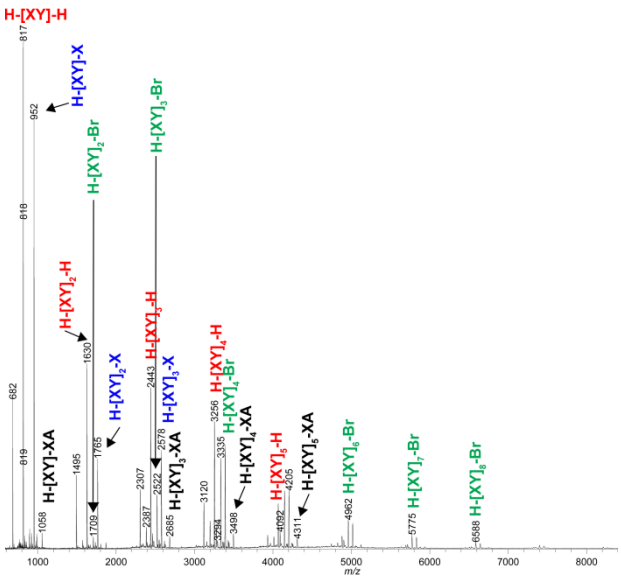

Figure-S 3 MALDI-TOF MS of **4**. X = 2,4-dimethylaniline, Y = diindenofluorene and A = anisole, Br = bromine.

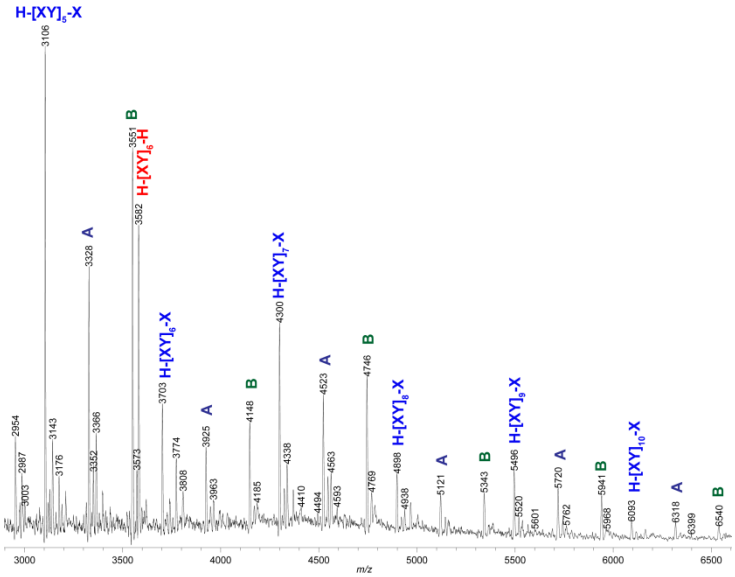

Figure-S 4 MALDI-TOF MS of **7**. X = 2,4-dimethylaniline, Y = indolocarbazole and A and B = series with unknown end-groups.

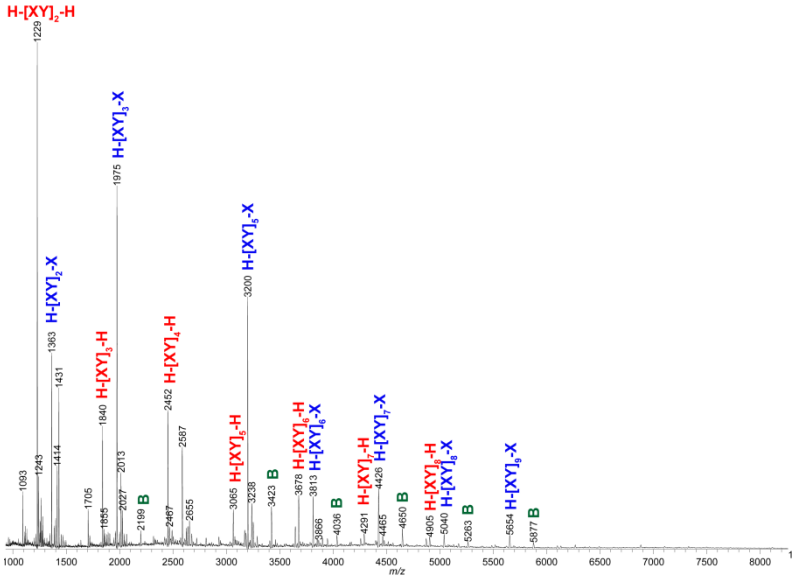

Figure-S 5 MALDI-TOF MS of **8**. X = 2-methyl-4-methoxy aniline, Y = indolocarbazole and B = series with unknown end-groups.

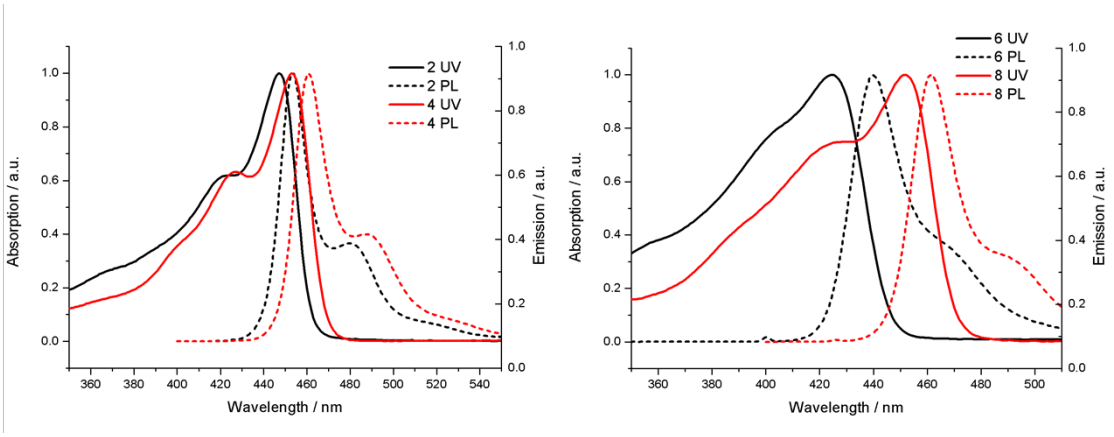

Figure-S 6 UV-Vis and PL spectra of polymer **2**, **4** (left) and **6**, **8** (right) in dichloromethane.

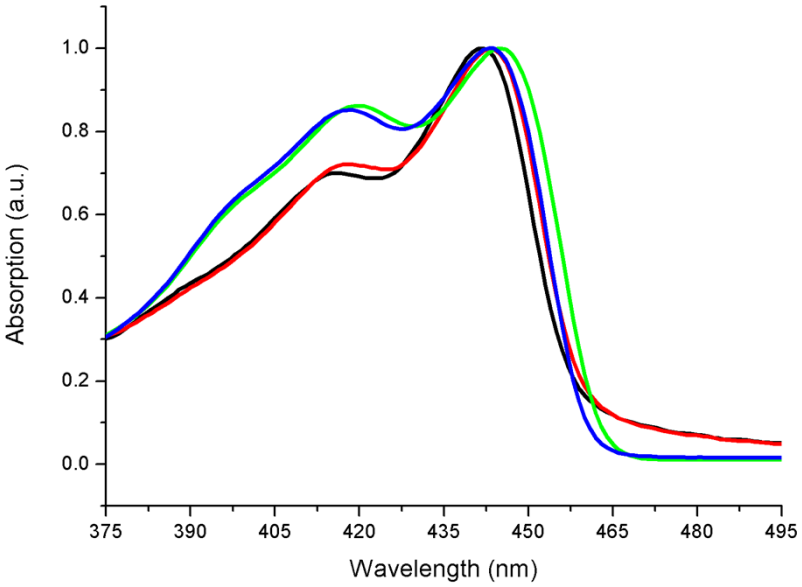

Figure-S 7 UV-Vis spectra of polymer **1** (black), **2** (red) and **3** (green), **4** (blue) as thin-films.

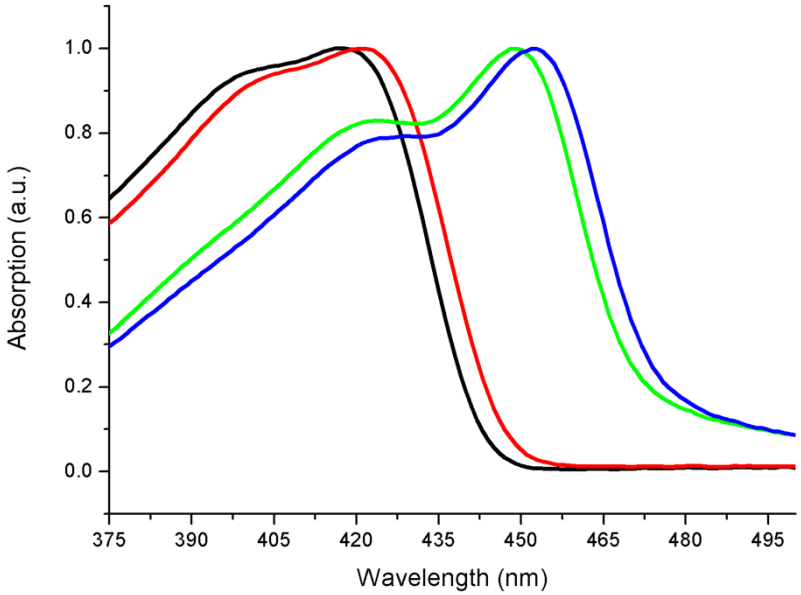

Figure-S 8 UV-Vis spectra of polymer **5** (black), **6** (red) and **7** (green), **8** (blue) as thin-films.

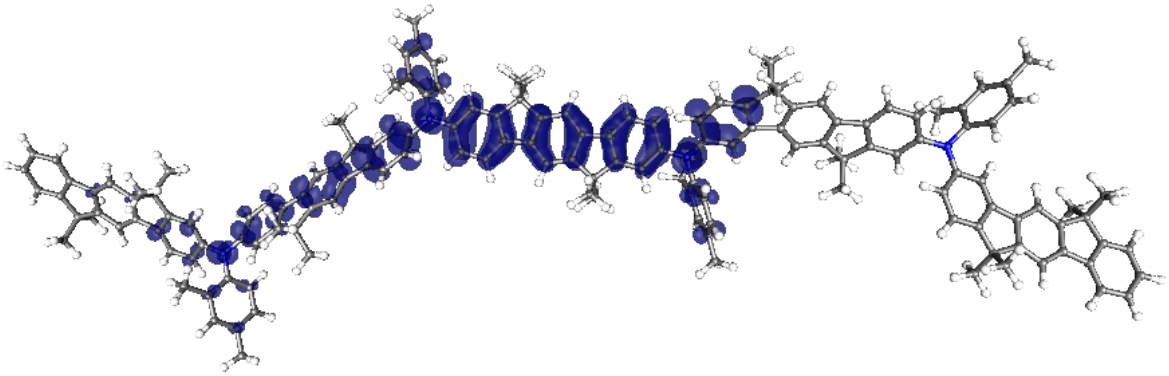

Figure-S 9 HOMO orbital tetramer **1**.

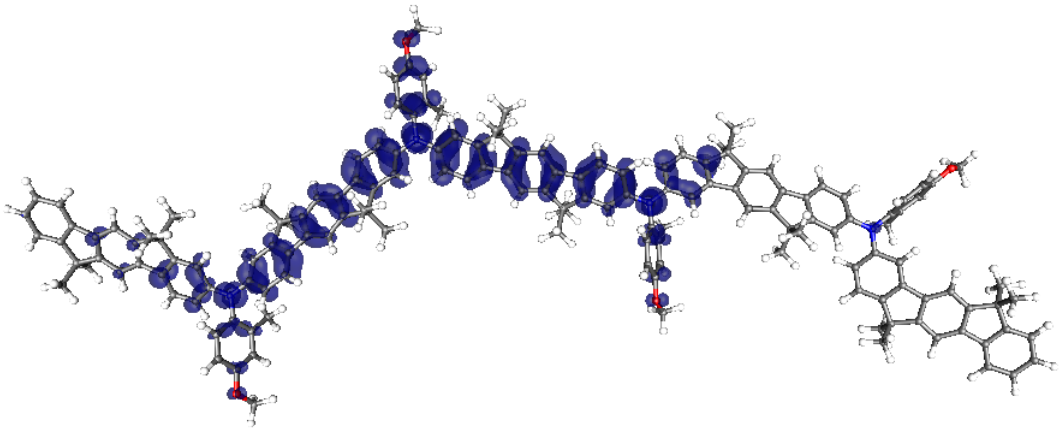

Figure-S 10 HOMO orbital tetramer **2**.

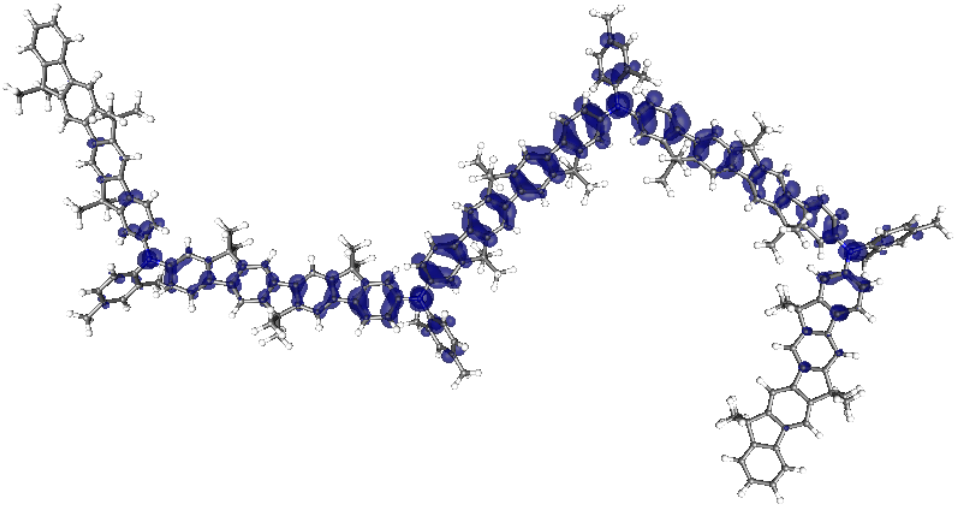

Figure-S 11 HOMO orbital tetramer **3**.

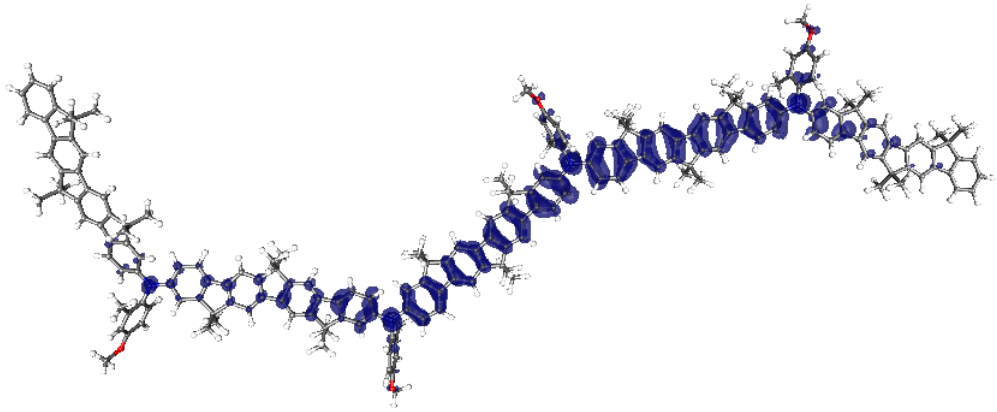

Figure-S 12 HOMO orbital tetramer **4**.

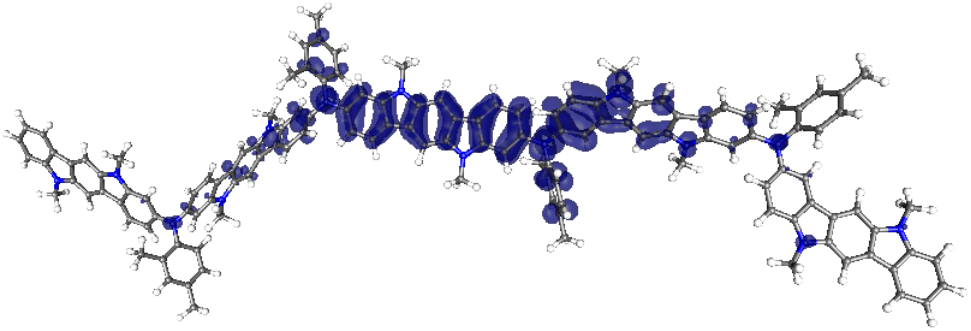

Figure-S 13 HOMO orbital tetramer **7**.

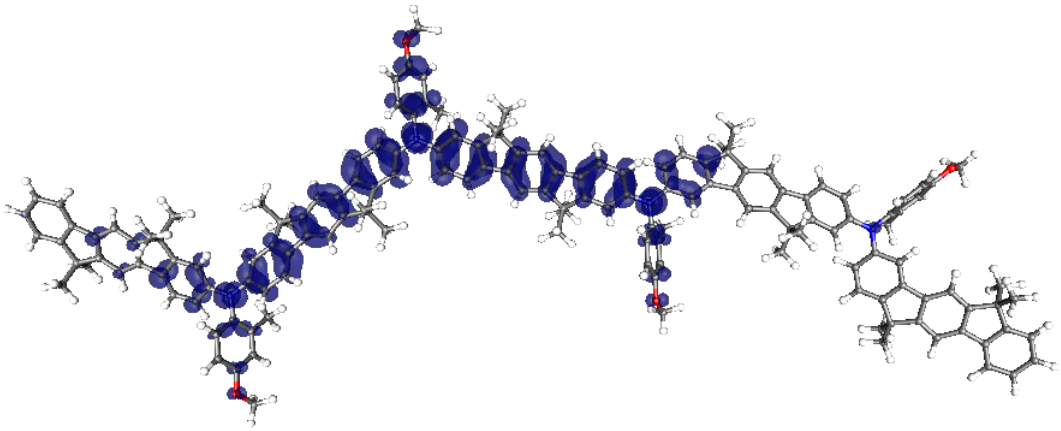

Figure-S 14 HOMO orbital tetramer **8**.

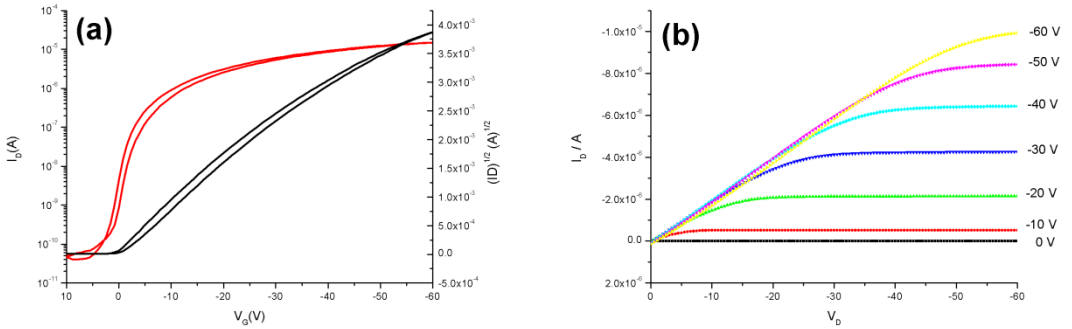

Figure-S 15 (a) Transfer Characteristics (L = 60 µm) and (b) Output Characteristics (L = 60 µm) for **1** in bottom gate / top contact devices on SiO_2/OTS.

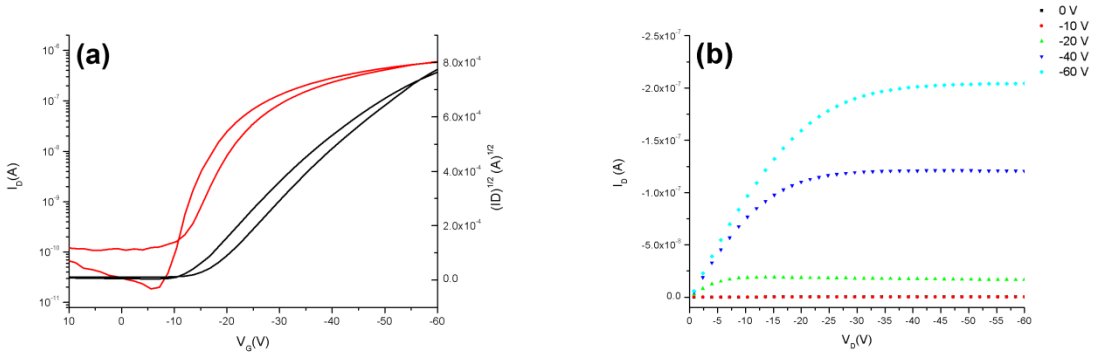

Figure-S 16 (a) Transfer Characteristics (L = 60 µm) and (b) Output Characteristics (L = 60 µm) for **2** in bottom gate / top contact devices on SiO_2/OTS.

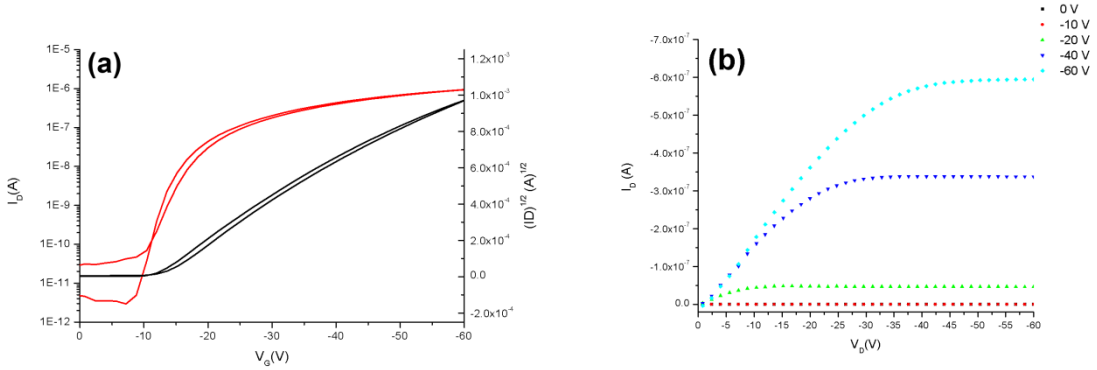

Figure-S 17 (a) Transfer Characteristics (L = 60 µm) and (b) Output Characteristics (L = 60 µm) for **3** in bottom gate / top contact devices on SiO_2/OTS.

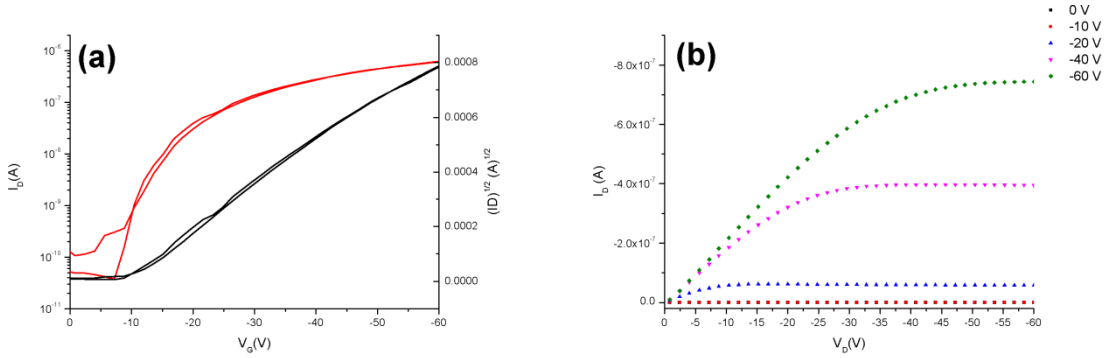

Figure-S 18 (a) Transfer Characteristics (L = 60 µm) and (b) Output Characteristics (L = 60 µm) for **4** in bottom gate / top contact devices on SiO_2/OTS.

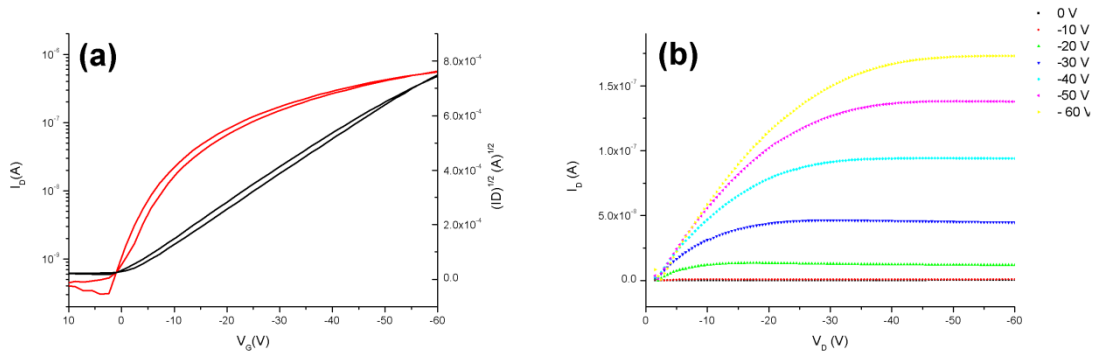

Figure-S 19 (a) Transfer Characteristics (L = 60 µm) and (b) Output Characteristics (L = 60 µm) for **5** in bottom gate / top contact devices on SiO_2/OTS.

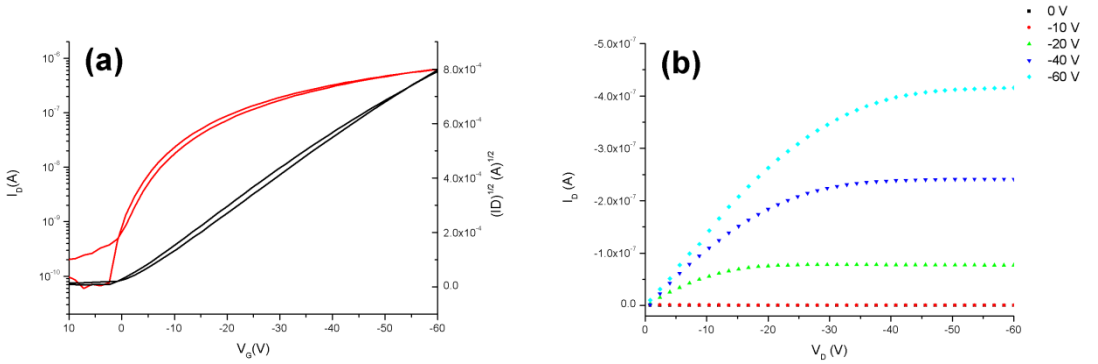

Figure-S 20 (a) Transfer Characteristics (L = 60 µm) and (b) Output Characteristics (L = 60 µm) for **6** in bottom gate / top contact devices on SiO_2/OTS.

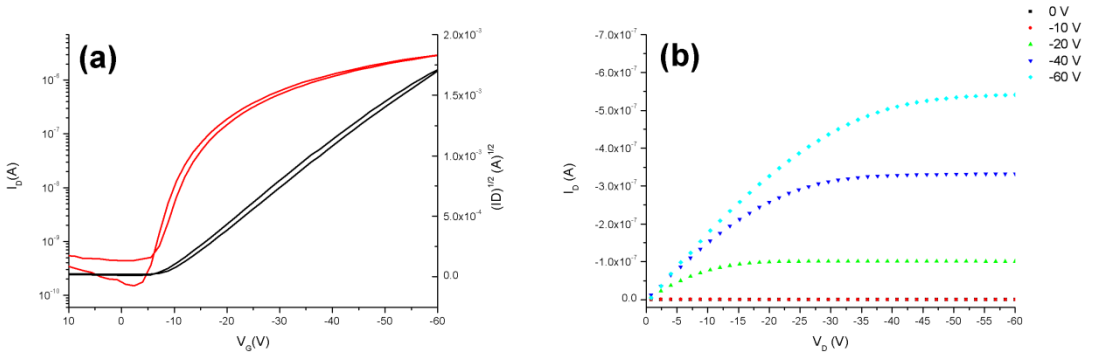

Figure-S 21 (a) Transfer Characteristics (L = 60 µm) and (b) Output Characteristics (L = 60 µm) for **7** in bottom gate / top contact devices on SiO_2/OTS.

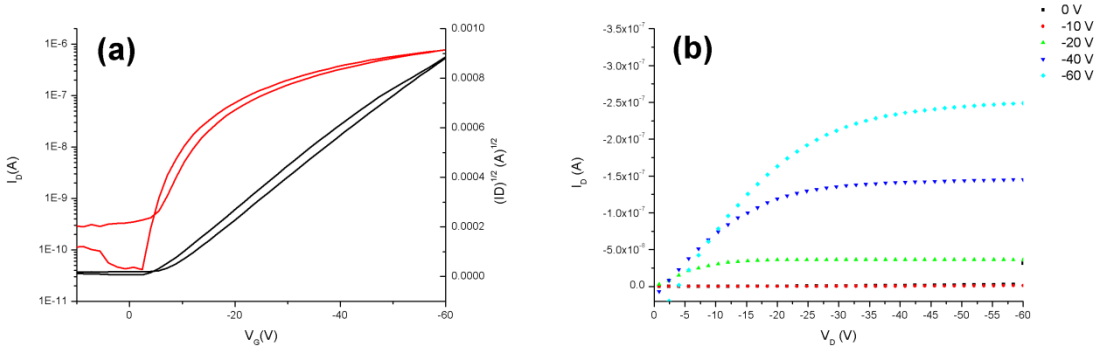

Figure-S 22 (a) Transfer Characteristics (L = 60 µm) and (b) Output Characteristics (L = 60 µm) for **8** in bottom gate / top contact devices on SiO_2/OTS.

S1 OFET Results

Polymer	***1***	***1 (Top-gated devices)***	***2***	***3***	***4***
Mobility / $cm^2 V^{-1} s^{-1}$	**$5.0 \times 10^{-2} \pm 8.1 \times 10^{-3}$** **$4.2 \times 10^{-2} \pm 1.1 \times 10^{-2}$**	**$5.1 \times 10^{-2} \pm 2.1 \times 10^{-3}$** **$5.0 \times 10^{-2} \pm 2.2 \times 10^{-3}$**	**$2.6 \times 10^{-3} \pm 3.4 \times 10^{-4}$** **$2.4 \times 10^{-3} \pm 2.2 \times 10^{-4}$**	**$3.5 \times 10^{-3} \pm 1.1 \times 10^{-4}$** **$2.9 \times 10^{-3} \pm 5.6 \times 10^{-4}$**	**$2.8 \times 10^{-3} \pm 2.5 \times 10^{-4}$** **$2.5 \times 10^{-3} \pm 3.6 \times 10^{-4}$**
V_{th} / V	-4 -4	-2 -2	-16 -15	-14 -10	-9 -8
Hysteresis	2 2	<1 <1	3 3	2 1	1 1
On/off	7×10^4 2×10^5	2×10^3 2×10^3	2×10^3 2×10^3	2×10^4 4×10^4	2×10^5 6×10^4
Working devices	6/9	4/4	7/9	8/9	8/9

Polymer	***5***	***6***	***7***	***8***
Mobility / $cm^2 V^{-1} s^{-1}$	**$1.1 \times 10^{-3} \pm 1.7 \times 10^{-5}$** **$1.0 \times 10^{-3} \pm 1.2 \times 10^{-4}$**	**$1.2 \times 10^{-3} \pm 1.3 \times 10^{-5}$** **$1.1 \times 10^{-3} \pm 6.7 \times 10^{-5}$**	**$3.7 \times 10^{-3} \pm 1.4 \times 10^{-3}$** **$2.8 \times 10^{-3} \pm 9.9 \times 10^{-4}$**	**$1.8 \times 10^{-3} \pm 2.2 \times 10^{-5}$** **$1.4 \times 10^{-3} \pm 3.3 \times 10^{-4}$**
V_{th} / V	-1 -2	-1 -2	-6 -6	-9 -9
Hysteresis	1 1	4 3	1 1	3 3
On/off	3×10^3 4×10^3	7×10^2 6×10^2	2×10^3 6×10^3	3×10^4 1×10^4
Working devices	9/9	6/9	9/9	8/9

Average of best 3 devices **Average of all working devices**

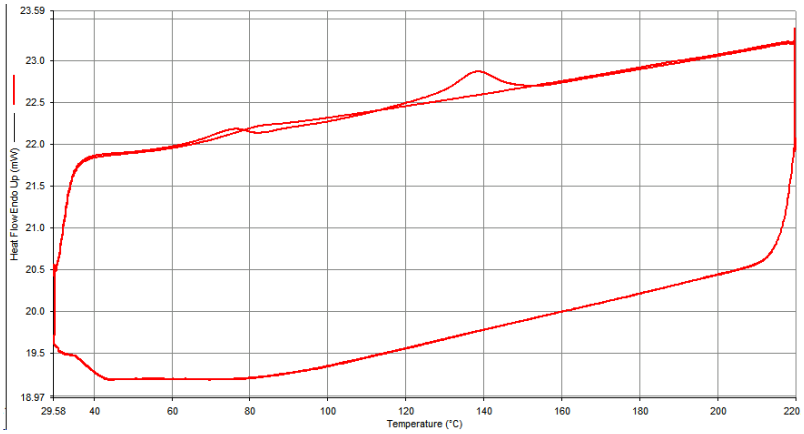

Figure-S 23 DSC of polymer **1** of the first and second cycle.

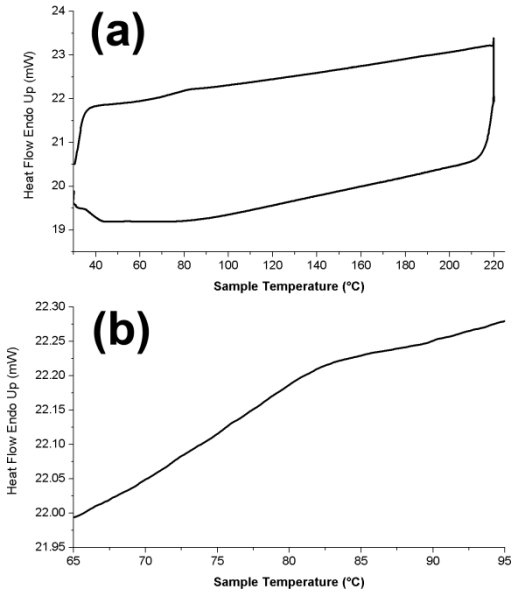

Figure-S 24 DSC of polymer **1**: (a) Second cycle, (b) expansion of the second cycle.

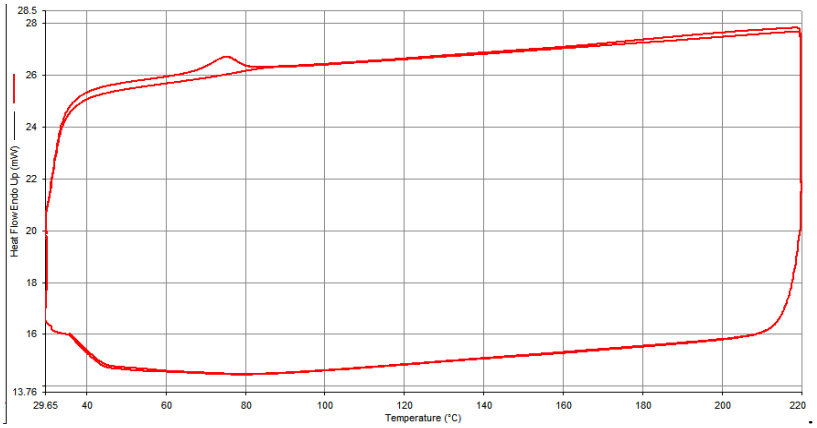

Figure-S 25 DSC of polymer **2**.

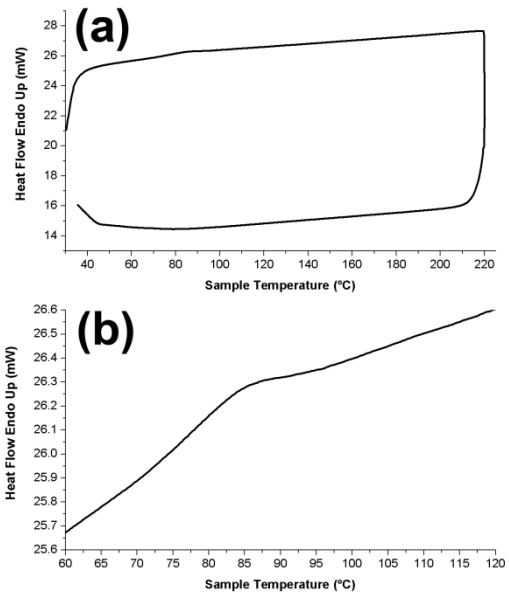

Figure-S 24 DSC of polymer **1**: (a) Second cycle, (b) expansion of the second cycle.

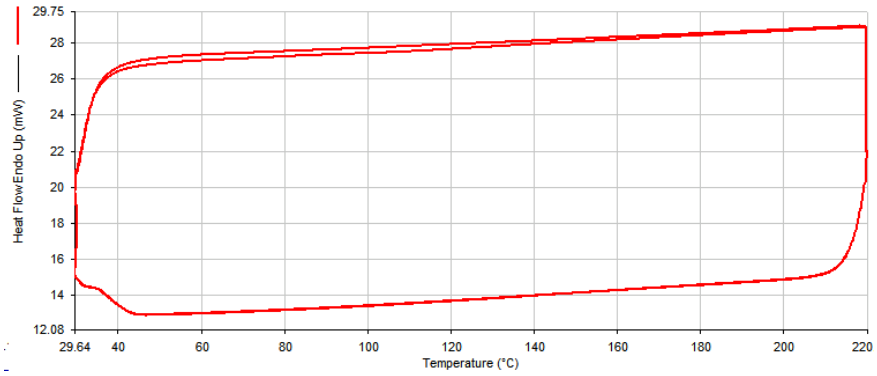

Figure-S 25 DSC of polymer **3**.

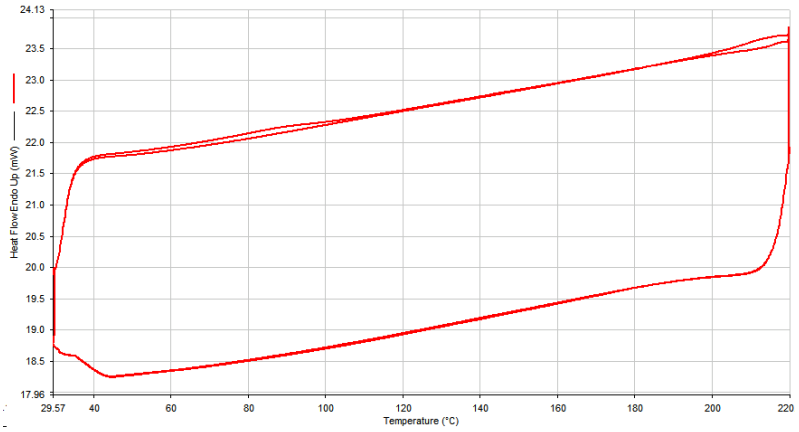

Figure-S 26 DSC of polymer **4**.

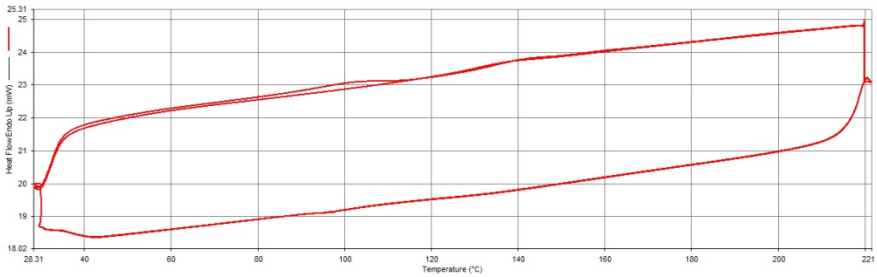

Figure-S 27 DSC of polymer **5**.

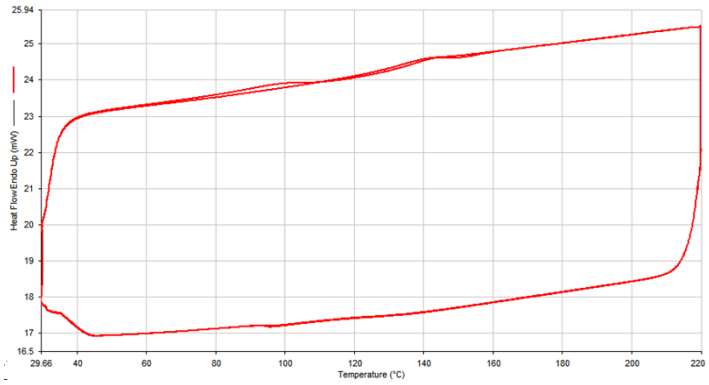

Figure-S 28 DSC of polymer **6**.

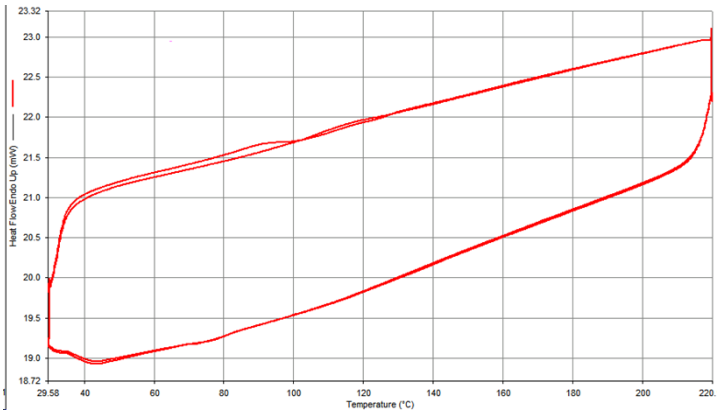

Figure-S 29 DSC of polymer **7**.

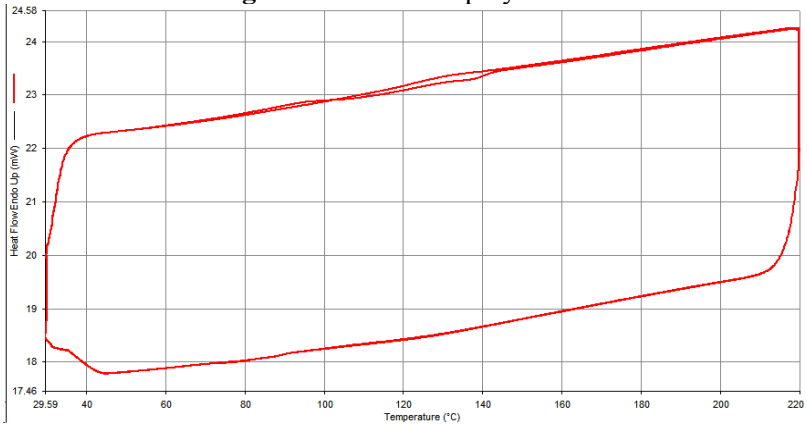

Figure-S 30 DSC of polymer **8**.

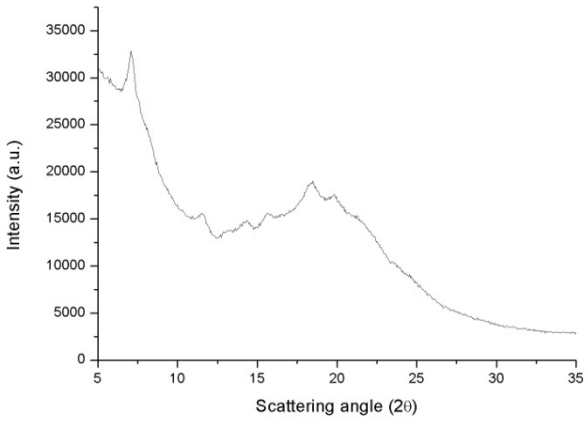

Figure-S 31 WAXS of polymer **1**.

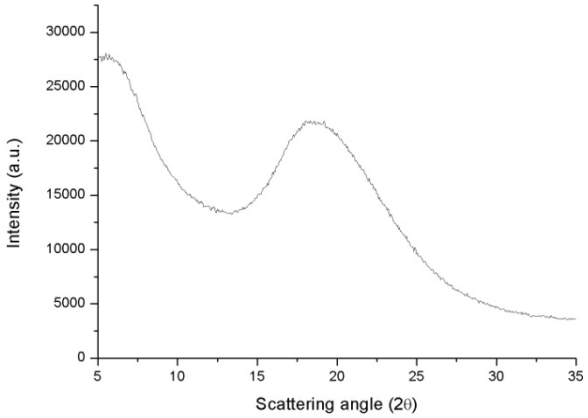

Figure-S 31 WAXS of polymer **2**.

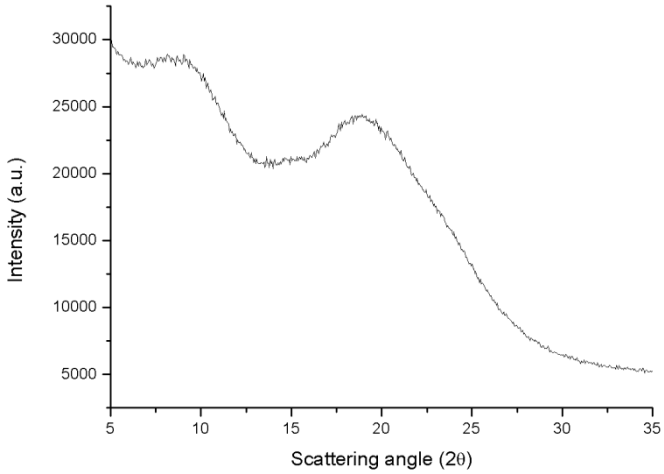

Figure-S 31 WAXS of polymer **3**.

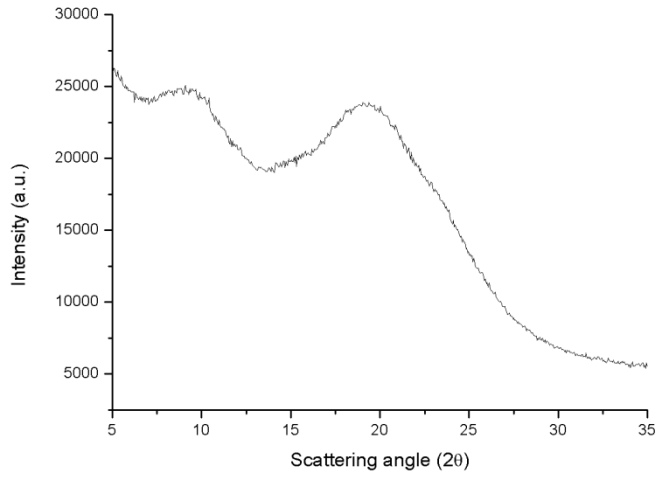

Figure-S 32 WAXS of polymer **4**.

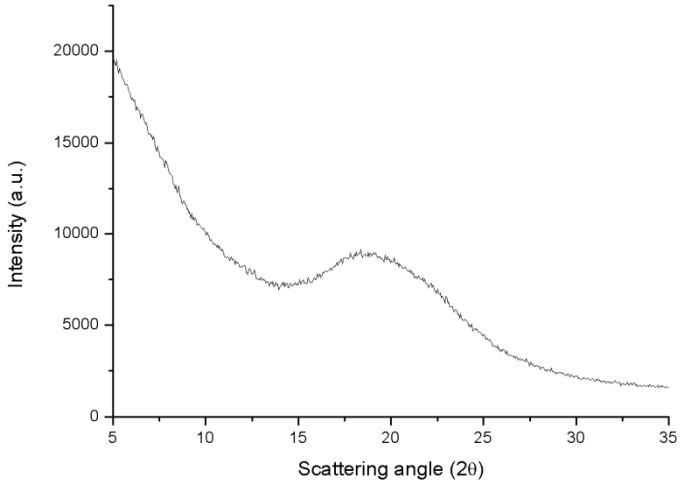

Figure-S 33 WAXS of polymer **7**.

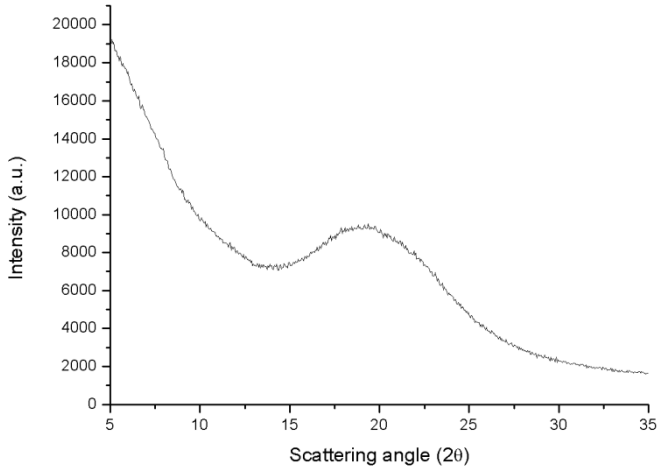

Figure-S 34 WAXS of polymer **8**.

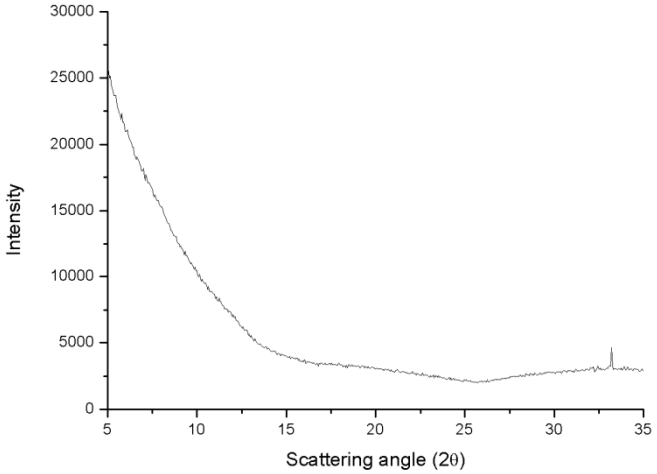

Figure-S 35 WAXS of polymer **1** deposited from TCE on OTS/SiO_2 dried 24 hours at 105 °C.

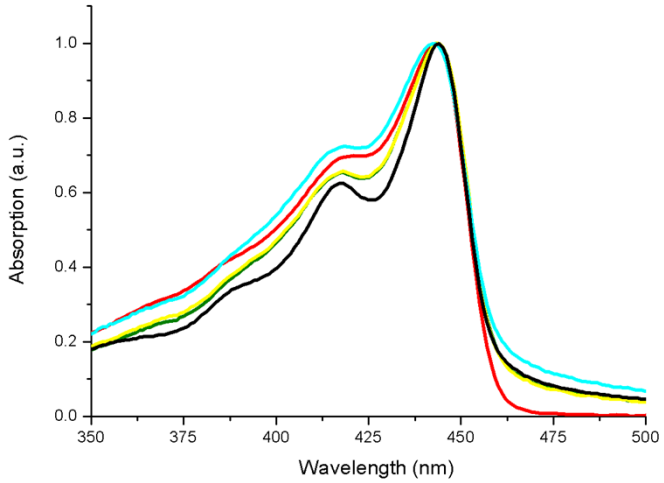

Figure-S 36 UV-Vis spectra of **1** in solution (red) and in thin film on glass (green), dried overnight at 105 ˚C (yellow), chlorobenzene vapor annealing at room temperature overnight (cyan) and chlorobenzene vapor annealing at 50 ˚C overnight (black).